4210 *Chem. Mater.* **2009,** *21,* 4210–4215
DOI:10.1021/cm900753f

CHEMISTRY OF MATERIALS
Article

Template Infiltration Routes to Ordered Macroporous TiN and SiN_x Films

Benjamin M. Gray,[†] Shereen Hassan,[†] Andrew L. Hector,*[,†] Ali Kalaji,[†,‡] and Baishakhi Mazumder[†]

[†] *School of Chemistry, University of Southampton, Southampton, U.K., and* [‡] *Present address: Department of Materials Science and Metallurgy, University of Cambridge, Pembroke Street, Cambridge CB2 3QZ, U.K.*

Received March 18, 2009. Revised Manuscript Received July 27, 2009

Ordered macroporous films of nanocrystalline TiN and amorphous SiN_x on silica substrates have been prepared. This involved infiltration of sacrificial templates of close-packed polystyrene microsphere arrays with precursor materials, followed by pyrolysis under ammonia to remove the template and form the ceramic materials. TiN was prepared from a sol−gel route, whereas SiN_x was introduced using a $Si(NHMe)_4$ precursor solution. Hexane was found to be the solvent most compatible with the divinylbenzene-cross-linked polystyrene template and was used for both materials.

Introduction

Ordered macroporous materials may be formed either as two-dimensional films or three-dimensional bulk structures. They have potential utility because of their periodic structures that can interact with light, uniform pore sizes that are large enough to allow liquids to diffuse readily, and high specific surface areas. Applications are in photonic band gap materials,[1] battery electrodes,[2] gas sensors,[3] optoelectronic devices,[4] catalysis,[5,6] membranes,[7,8] and biomaterials.[9] These materials are usually synthesized using arrays of close-packed spheres as templates[10] (typically of silica or polystyrene); the void space between the spheres is infiltrated with precursors of the target material. Upon removal of the template spheres (by thermal processing, solvent extraction, or chemical etching), ordered inverse opal structures are obtained.

So far, attention has focused mainly on ceramic macroporous structures of binary oxides such as SiO_2, TiO_2, Al_2O_3, ZrO_2,[11,12] and ternary transition/main-group metal oxides,[13] as well as organic polymers,[8,14] semiconductors,[15] and carbon.[2] However, there are only a few examples of templated porous nitride materials. Inverse opals of WN[16] and Ta_3N_5[17] have been produced by atomic layer deposition (ALD) through a silica template. This method was found suitable for making Ta_3N_5 with a photonic band gap at optical wavelengths. While ALD yields extremely high quality materials, it is expensive, time-consuming and not suitable for yielding bulk structures. High-quality photonic crystals of GaN have been prepared by opal-SiO_2 templating with Ga_2O_3 followed by annealing in an atmosphere of nitrogen hydrides.[18] Ordered macroporous SiCN has been formed by templating silica spheres with a preceramic precursor, polysilazane.[6] The material obtained is promising as a catalyst support for high-temperature fuel reforming because of its surface geometry and good stability up to 1200 °C. High-surface-area mesoporous boron nitride was synthesized by nanocasting mesoporous carbon with a molecular boron nitride precursor.[19]

*Fax: (44)2380596805. Tel: (44)2380594125. E-mail: A.L.Hector@soton.ac.uk.

(1) Norris, D. J.; Vlasov, Y. A. *Adv. Mater.* **2001**, *13*, 371. Stein, A.; Li, F.; Denny, N. R. *Chem. Mater.* **2008**, *20*, 649.
(2) Lee, K. T.; Lytle, J. C.; Ergang, N. S.; Oh, S. M.; Stein, A. *Adv. Funct. Mater.* **2005**, *15*, 547.
(3) Scott, R. J. W.; Yang, S. M.; Chabanis, G.; Coombs, N.; Williams, D. E.; Ozin, G. A. *Adv. Mater.* **2001**, *13*, 1468. Acciarri, M.; Barberini, R.; Canevali, C.; Mattoni, M.; Mari, C. M.; Morazzoni, F.; Nodari, L.; Polizzi, S.; Ruffo, R.; Russo, U.; Sala, M.; Scotti, R. *Chem. Mater.* **2005**, *17*, 6167.
(4) Mihi, A.; Míguez, H. *J. Phys. Chem. B* **2005**, *109*, 15968. Imada, M.; Noda, S.; Chutinan, A.; Tokuda, T. *Appl. Phys. Lett.* **1999**, *75*, 316.
(5) Carreon, M. A.; Guliants, V. V. *Chem. Mater.* **2002**, *14*, 2670. Al-Daous, M. A.; Stein, A. *Chem. Mater.* **2003**, *15*, 2638.
(6) Sung, I.-K.; Christian, M. M.; Kim, D.-P.; Kenis, P. J. A. *Adv. Funct. Mater.* **2005**, *15*, 1336.
(7) Park, S. H.; Xia, Y. *Adv. Mater.* **1998**, *10*, 1045.
(8) Gates, B.; Yin, Y.; Xia, Y. *Chem. Mater.* **1999**, *11*, 2827.
(9) Yan, H.; Zhang, K.; Blanford, C. F.; Francis, L. F.; Stein, A. *Chem. Mater.* **2001**, *13*, 1374. Melde, B. J.; Stein, A. *Chem. Mater.* **2002**, *14*, 3326. Zhang, K.; Yan, H.; Bell, D. C.; Stein, A.; Francis, L. F. *J. Biomed. Mater. Res.* **2003**, *66A*, 860.
(10) Xia, Y.; Gates, B.; Yin, Y; Lu, Y. *Adv. Mater.* **2000**, *12*, 693.
(11) Abdullah, M.; Iskandar, F.; Shibamoto, S.; Ogi, T.; Okuyama, K. *Acta Mater.* **2004**, *52*, 5151. Carreon, M. A.; Guliants, V. V. *Eur. J. Inorg. Chem.* **2005**, 27.
(12) Carbajo, M. C.; Gómez, A.; Torralvo, M. J.; Enciso, E. *J. Mater. Chem.* **2002**, *12*, 2740.
(13) Madhavi, S.; Ferraris, S.; White, T. *J. Solid State Chem.* **2006**, *179*, 866.
(14) Ghanem, M. A.; Bartlett, P. N.; de Groot, P.; Zhukov, A. *Electrochem. Commun.* **2004**, *6*, 447.
(15) Meseguer, F.; Blanco, A.; Míguez, H.; García-Santamaría, F.; Ibisate, M.; López, C. *Colloids Surf., A* **2002**, *202*, 281. Vlasov, Y. A.; Bo, X.-Z.; Sturm, J. C.; Norris, D. J. *Nature* **2001**, *414*, 289.
(16) Rugge, A.; Becker, J. S.; Gordon, R. G.; Tolbert, S. H. *Nano Lett.* **2003**, *3*, 1293.
(17) Rugge, A.; Park, J.-S.; Gordon, R. G.; Tolbert, S. H. *J. Phys. Chem. B* **2005**, *109*, 3764.
(18) Gajiev, G.; Golubev, V. G.; Kurdyukov, D. A.; Pevtsov, A. B.; Selkin, A. V.; Travnikov, V. V. *Phys. Status Solidi B* **2002**, *231*, R7.
(19) Dibandjo, P.; Chassagneux, F.; Bois, L.; Sigala, C.; Miele, P. *Micro. Meso. Mater.* **2006**, *92*, 286.

Published on Web 08/27/2009

There is a clear need to develop routes to other nitride materials, as their properties vary significantly from those of oxides and new macroporous metallic, semiconductor or insulator nitride compositions will be of significant interest. Very recently some progress in this was demonstrated by Fischer et al.,[20] who infiltrated a template of 60 nm silica spheres with molten cyanamide and pyrolyzed to make a macroporous graphitic C_3N_4 powder. After dissolution of the SiO_2 spheres, $TiCl_4$ and ethanol were infiltrated and samples were fired under N_2 at 800 °C to yield TiN/amorphous carbon nanocomposite powders, in which TEM showed that an ordered macroporous structure was maintained. These authors suggested application of the porous metal nitride as a catalyst or catalyst support. However, applications as electrodes could be envisaged for high surface area films of such an inert yet highly conductive material.[21,22] The photocatalytic properties are also likely to be of interest if the surface is oxidized to highly photoactive TiO_2.[23]

Sol−gel synthesis has the potential to yield nitride materials in various useful morphologies.[24] Infiltration of a precursor or templating of a sol−gel process are the routes used to produce many of the macroporous oxides described above,[13,25] but there are few examples of templating processes to yield nitrides. Microporous silicon nitride has been prepared using sol−gel templating on long chain amines and showed a higher selectivity over nontemplated silicon nitride in the catalysis of alkylation and isomerization reactions.[26] A number of porous silicon nitride structures have also been prepared using sol−gel chemistry without a template, including high-surface-area aerogels,[27] membranes,[28,29] and mesoporous powders.[30] Sol−gel processes have also been used to obtain titanium nitride materials. Nitridation of sol−gel-derived TiO_2 has led to TiN fibers.[31] Films[32,33] and nanocrystalline powders[34] of TiN have also been synthesized using sol−gel chemistry.

In this work, we aim to extend the synthesis of ordered macroporous templated nitride materials. We report on the synthesis of inverse opal films of insulating silicon nitride (SiN_x) and metallic titanium nitride (TiN) formed by infiltrating templates of close-packed 500 nm polystyrene spheres with precursor solutions and sols. The method described herein is simple yet effective for yielding new nitride materials with the inverse opal morphology. Because infiltration is carried out from nonaqueous solutions, it could also have more general applicability to nonoxide materials.

Experimental Section

All sol preparations and infiltrations were carried out under dry N_2 conditions using a glovebox or Schlenk line. Silica tiles for coating were cleaned with piranha etch (1:3 H_2SO_4:H_2O_2) and then rinsed thoroughly with distilled water and dried. Thin film arrays of polystyrene (PS) spheres were generated as follows: An aqueous solution of divinylbenzene-cross-linked, amidine-capped polystyrene microspheres (4%, 500 ± 17 nm, Invitrogen) was sonicated for 15 min and then diluted to 1% with deionized water. This solution (0.15 cm^3 per array) was syringed into PTFE wells (diameter 7 mm) sealed onto the surface of the silica tiles by clamping between stainless steel plates. These were allowed to evaporate in a refrigerator (∼4 °C) over 7−10 days yielding iridescent green arrays.

Of the various solvents used to produce sols and solutions for templating the arrays, hexane caused the least interference with the array structure and yielded the best results. $Ti(NMe_2)_4$ (3 cm^3, 11.2 mmol, Epichem) was dissolved in dry hexane (7.5 cm^3, distilled from sodium/benzophenone). $^nPrNH_2$ (1.75 cm^3, 22.4 mmol, distilled from BaO) was slowly added. The solution was stirred at room temperature for ∼16 h, during which time it turned opaque and a brick-red precipitate formed (within 30 min) and subsequently dissolved giving a homogeneous blood-red sol. The sol was infiltrated into the PS arrays by placing the tiles into the sol at an angle so that the level of the sol was just touching the edge of the array. The tiles were left to stand in the sol for 45 min, then removed and allowed to dry for 2 h. The infiltrated arrays were heated under a flow of dry ammonia to 600 °C at 2.5 °C min^{-1} and maintained for 10 h. Using these conditions, heating PS arrays under NH_3 completely removed the PS without leaving any residue. A sol prepared as above yielded a viscous red gel upon removal of the solvent under a vacuum. This gel was also heated under ammonia as described above to yield a block of material that was ground to a dark-red TiN powder.

SiN_x macroporous arrays were produced by direct infiltration of a precursor. The precursor used, $Si(NHMe)_4$, was synthesized from $SiCl_4$ and methylamine (both 99%, Aldrich) in n-pentane and then purified by sublimation (45 °C). A solution of $Si(NHMe)_4$ (0.5 g, 3.4 mmol) in dry hexane (6 cm^3) was used to infiltrate the arrays by fully immersing the array-coated tiles into the precursor solution and then allowing them to dry for 15 min. The arrays were heated under dry ammonia to 50 at 0.5 °C min^{-1} and maintained for 1 h, then finally to 500 at 1 °C min^{-1} and maintained for 1 h. Samples of bulk $Si(NHMe)_4$ were also pyrolyzed under ammonia in the same manner to yield white SiN_x powder.

Scanning electron microscopy (SEM) was carried out using a JEOL JSM-5910 microscope coupled with an Oxford Inca 300 X-ray detector (energy dispersive X-ray (EDX) microanalysis). The EDX probe was insensitive to N because of a BN window,

(20) Fischer, A; Jun, Y.-S.; Thomas, A.; Antonietti, M. *Chem. Mater.* **2008**, *20*, 7383.
(21) Kirchner, C. N.; Halmeier, K. H.; Szargan, R.; Raschke, T.; Radehaus, C.; Wittstock, G. *Electroanalysis* **2009**, *19*, 1023.
(22) Choi, D.; Kumta, P. N. *J. Electrochem. Soc.* **2006**, *153*, A2298.
(23) Selli, E.; Chiarello, G. L.; Quartarone, E.; Mustarelli, P.; Rossetti, I.; Forni, L. *Chem. Commun.* **2007**, 5022.
(24) Hector, A. L. *Chem. Soc. Rev.* **2007**, *36*, 1745. Mazumder, B; Hector, A. L. *J. Mater. Chem.* **2009**, *19*, 4673.
(25) Lytle, J. C.; Stein, A. Recent progress in syntheses and applications of inverse opals and related macroporous materials prepared by colloidal crystal templating. In *Annual Reviews of Nano Research* Cao, G., Brinker, C. J., Eds.; World Scientific Publishing Co.: River Edge, NJ, 2006; Vol. *1*, pp 1−79 and references therein.
(26) Farruseng, D.; Schlichte, K.; Spliethoff, B.; Wingen, A.; Kaskel, S.; Bradley, J. S.; Schüth, F. *Angew. Chem., Int. Ed.* **2001**, *40*, 4204.
(27) Hassan, S.; Hector, A. L.; Hyde, J. R.; Kalaji, A.; Smith, D. C. *Chem. Commun.* **2008**, 5304.
(28) Cheng, F.; Kelly, S. M.; Clark, S.; Bradley, J. S.; Baumbach, M.; Schütze, A. *J. Membr. Sci.* **2006**, *280*, 530.
(29) Völger, K. W.; Hauser, R.; Kroke, E.; Riedel, R.; Ikuhara, Y. H.; Iwamoto, Y. *J. Ceram. Soc. Jpn.* **2006**, *114*, 567.
(30) Cheng, F.; Clark, S.; Kelly, S. M.; Bradley, J. S. *J. Am. Ceram. Soc.* **2004**, *87*, 1413.
(31) Kamiya, K.; Yoko, T.; Bessho, M. *J. Mater. Sci.* **1987**, *22*, 937.
(32) Jackson, A. W.; Hector, L. *J. Mater. Chem.* **2007**, *17*, 1016.
(33) Ezz, T.; Crouse, P.; Li, L.; Liu, Z. *Appl. Surf. Sci.* **2007**, *253*, 7903.
(34) Jackson, A. W.; Shebanova, O.; Hector, A. L.; McMillan, P. F. *J. Solid State Chem.* **2006**, *179*, 1383. Kim, I.-S.; Kumta, P. N. *Mater. Sci. Eng., B* **2003**, *98*, 123.

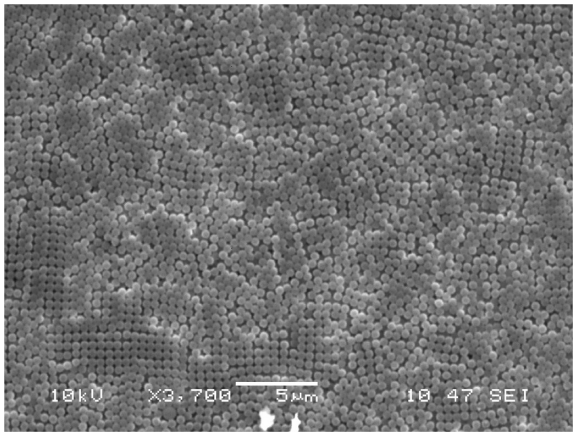

Figure 1. SEM micrograph of an array of DVB cross-linked PS microspheres displaying regions of close-packing.

so EDX was used mainly to probe incorporation of other impurities; none were observed. SEM samples were mounted on a conductive stub and coated with carbon or gold. Powder X-ray diffraction (PXD) data were collected using a Siemens D5000 diffractometer with Cu-$K_{\alpha 1}$ radiation. Rietveld refinements were carried out using the GSAS package.[35] A Bruker D8 Discover with Gadds diffractometer was used for XRD on films, these were measured with a 5° incident angle. Fourier transform−infrared (FT-IR) spectra were collected using a Perkin-Elmer Spectrum One FT-IR spectrometer. The samples were pressed into discs with dry CsI and placed into an inert atmosphere holder for measurement. Raman spectra were recorded with a Perkin-Elmer FT Raman 2000R using a Nd:YAG laser.

Thermogravimetric analysis (TGA) was performed with a glovebox mounted Mettler Toledo TGA/SDTA 851e. TGA samples (10−20 mg) were heated under flowing high purity nitrogen (Air Products BiP grade, 50 cm^3 min^{-1}) at a rate of 9 °C min^{-1} to 800 °C and maintained for 1 h. Combustion (C, H, N) analysis was carried out commercially by MEDAC Ltd. Differential scanning calorimetry (DSC) was performed on a Mettler Toledo DSC 821e using a 1.77 mg sample in a 40 μL aluminum crucible.

Results and Discussion

The arrays of PS spheres were examined by SEM to reveal polycrystalline lattices with close-packed domains and some amorphous regions (Figure 1). These templates were deemed acceptable for our proof-of-concept investigations of templating macroporous nitride materials. Templates with long-range order could be obtained from the same spheres if required by changing the array deposition conditions.[10,12,36] The diameters of the spheres are confirmed by SEM to be 500 nm. DSC showed that the PS polymer has a glass transition temperature at ~110 °C, but does not melt below 300 °C. This is important because the infiltrated material will cross-link as the temperature is raised under ammonia flow and needs to become rigid before the template structure is disrupted.

Macroporous TiN

Templated TiO_2 is relatively straightforward to make because sols can be produced in alcohol/water mixtures, so our investigation started with an attempt to convert ordered macroporous films of TiO_2 into TiN by high-temperature ammonolysis. The titania arrays were prepared according to a method described by Carbajo et al.[12] using the PS arrays described above as templates. The conversion by ammonolysis was initially attempted at 800 °C for 20 h, which was expected to yield titanium oxynitride according to a previous report.[37] Under these conditions a total loss of the porous structure was observed. Complete conversion to TiN requires temperatures in excess of 1000 °C,[31] so this route to macroporous TiN is not feasible. A method involving ammonolysis under milder conditions is necessary for making templated macroporous TiN and a nonoxide sol−gel method based on an amide precursor was the obvious choice.

The choice of solvent for this method is crucial for preserving the structure of the PS template. Oxides can be templated around most types of polymer spheres because the chemistry can be carried out in compatible solvents such as alcohols. Most nonoxide sol−gel work for nitrides has used THF as the solvent[27,28,30,32] as high polarity solvents usually displace amide groups and low polarity solvents do not solubilize the sol particles. The cross-linked PS particles were found to be much more solvent resilient than standard polystyrene but THF was still found to dissolve the arrays, as was toluene. Initially, sol−gel infiltrations were carried out in diethylamine because sol formation proceeded smoothly yielding homogeneous, translucent solutions for infiltration. However, it was later found that even though PS arrays treated with diethylamine did not dissolve, they lost their iridescence, indicating a disruption in their structures. This was also observed for diethyl ether. Hexane had no effect on the arrays, the iridescence remaining intact even after soaking in hexane for 2 h. Hence the key to producing good macroporous arrays was to form the sols in hexane or another very low polarity solvent. Similarly, the capping agent on the polymer spheres needs to be as compatible as possible with the precursor chemistry; here, amidine-capped spheres were used.

Previously, we showed that $Ti(NMe_2)_4$ reacts with various primary amines in THF solution to yield sols that can be used to produce TiN films on glass.[32] Here *n*-propylamine was chosen as the cross-linking agent and sol formation was attempted in various solvents. In benzene, toluene, diethylamine, and diethyl ether, sols formed in the same way as they do in THF, a red color slowly develops from the yellow precursor solution and becomes darker with a small increase in solution viscosity. The sols could also be formed at much higher concentrations than used in the previous paper, which is important in order to maximize the density of the material in the final array. In hexane, the formation of a precipitate is

(35) Larson, A. C.; Von Dreele, R. B. *General Structure Analysis System (GSAS)*; Los Alamos National Laboratory Report LAUR 86−748; Los Alamos National Laboratory: Los Alamos, NM, 2004.
(36) Zhao, X. S.; Su, F.; Yan, Q.; Guo, W.; Bao, X. Y.; Lv, L.; Zhou, Z. *J. Mater. Chem.* **2006**, *16*, 637.
(37) Clarke, S. J.; Michie, C. W.; Rosseinsky, M. J. *Chem. Mater.* **2000**, *12*, 863.

Scheme 1

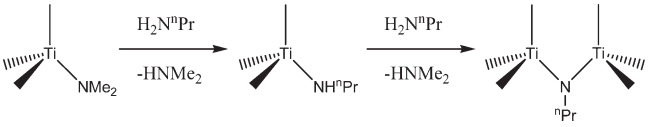

observed in the early stages of the reaction (following addition of $^{n}PrNH_2$), which later dissolves. The first step of the reaction is transamination leading to Ti-NH^{n}Pr groups, which may be of low solubility in hexane because of the rather polar N−H. As self-condensation reactions proceed with other titanium centers, these polar groups are eliminated forming oligomeric particles with Ti−N^{n}Pr−Ti cross-linkages (Scheme 1). These could be expected to be more soluble in hexane, which would explain the redissolution and formation of a stable colloidal suspension.

Various methods for templating the TiN_x hexane sols were tried, including dipping or soaking the PS arrays in the sol and dropping the sol onto the array and leaving to evaporate in the glovebox. The method of infiltration described in the Experimental Section gave the best structures postammonolysis as imaged by SEM. Ammonolysis was carried out at 600 °C and heating to higher temperatures (700 and 800 °C) caused the ordered macroporous structure to collapse. It is clear from the images obtained that the ammonolysis succeeded in the removal of the PS spheres while preserving the templated porous structure of TiN. Figure 2 shows the typical features of the macroporous films produced. As observed in the templates, ordered domains or pores are observed. Many of the templated films were also opalescent, appearing green from certain directions, which is also an indication of a high level of overall order. Some cracking is observed beyond that, which can be attributed to imperfections in the PS template. Looking down a crack in the film, it can be seen that the porosity extends through the several micrometers thickness. Further, pores are also visible from the main surface from beneath the top layer. These observations imply that the porosity extends throughout the structure. In the ~7 μm thick film shown in Figure 2 the surface area can be calculated from simple geometry as ca. 62 cm^2 per cm^2 of film, though there is no reason why the film thickness could not be increased.

It is difficult to obtain good-quality analytical data directly on these films, as they are of low density and most methods observe the substrate as well as the film. Hence a bulk xerogel was also produced by ammonolysis of a sample produced by evaporating one of the sols used for infiltration under the same conditions as the films. PXD showed the sample to be TiN and Rietveld refinement produced a lattice parameter of 4.2281(13) Å, which is close to literature values for TiN.[38] The crystallite size can be extracted from the Lorentzian broadening of the diffraction peaks if an instrumental function is first refined to fix the Gaussian part of the peak shape,[35] this procedure yields a crystallite size of 7 nm. The refined pattern is shown in Figure 3. Minimal amorphous scattering is observed from this sample, in contrast to similar xerogels crystallized at similar temperatures in our previous study.[32] Here the xerogels were made from the sols with a restricted amount of cross-linking agent, whereas previously an excess of amine was added to induce precipitation and it was that precipitate which was fired. The smaller oligomer size that would result from the current method may produce a xerogel that crystallizes more readily and hence these samples were mainly nanocrystalline rather than a mixture of nanocrystals and significant amounts of amorphous material.

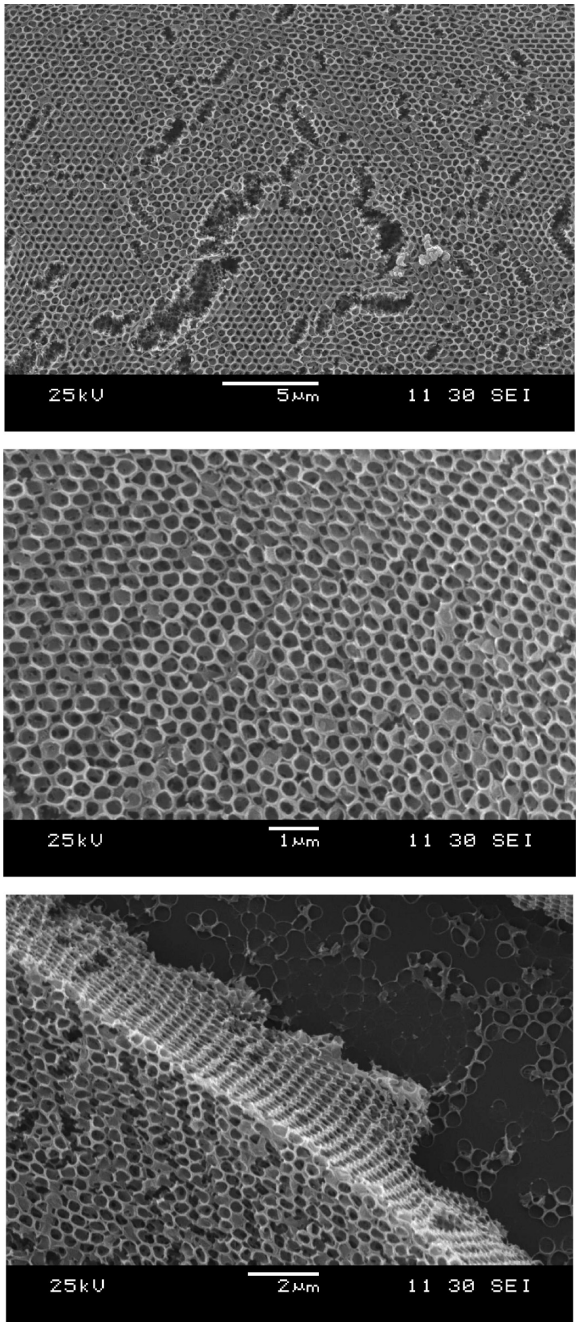

Figure 2. SEM micrographs of thin films of ordered macroporous TiN on a silica substrate showing cracking of the films (top), ordering of pores within a domain (center), and the view down a large crack in the film showing pores lining the walls.

(38) *PCPDFWIN Powder Diffraction File*, version 2.4; International Center for Diffraction Data: Swarthmore, PA, 2003.

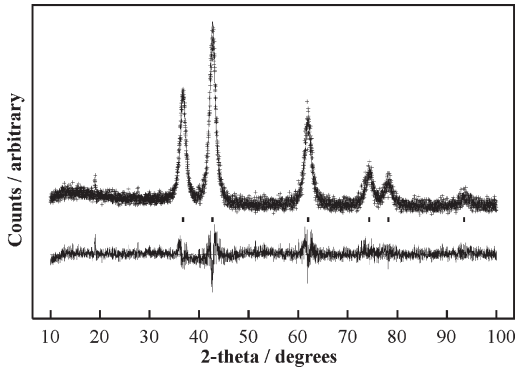

Figure 3. X-ray diffraction data of TiN powder produced from ammonolysis of the TiN_x gel at 600 °C. Crosses mark the data points, the upper continuous line the Rietveld profile fit and the lower continuous line the difference. Tick marks show the positions of allowed reflections in the TiN structure in space group $Fm\bar{3}m$.

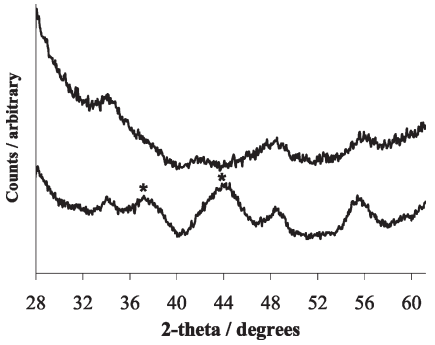

Figure 4. X-ray diffraction data of a macroporous TiN film. The top trace shows a blank silica tile collected in the same geometry as the bottom trace, where the tile was the substrate for the film. The extra features in the bottom trace marked by asterisk correspond to the 111 and 200 reflections of TiN.

FT-IR studies show ν_{C-H} bands at 2960−2760 cm^{-1} for the TiN_x gel, which disappear on ammonolysis to TiN powder. The absence of ν_{N-H} in the gel indicates that the reaction of $Ti(NMe_2)_4$ with $^nPrNH_2$ led almost exclusively to Ti−N^{n}Pr−Ti linkages by the time the solvent had evaporated, hence the gels are then insoluble. Ammonolysis at 600 °C removes alkyl groups (ν_{C-H}) from the structure, through substitution of propylamine and dimethylamine by ammonia or by β-hydride elimination. TGA shows minimal (< 2%) weight loss on heating these powders to 800 °C. Very little carbon impurity is left in the product, microanalysis shows 18.6% N, 0.8% C, and < 0.1% H (TiN theoretical 22.6% N).

The macroporous films scatter X-rays very weakly due to the porous structure and a significant background is observed due to the silica substrate. Collecting patterns for an extended period with a low (5°) incident angle, peaks can be observed at 36.7 and 42.6° because of crystalline TiN, Figure 4, with a = 4.21 Å. Analysis of the line width using the Scherrer formula[39] and comparing with an Al standard collected with the same incident beam angle suggests the same crystallite size to that found in the bulk xerogel (7 nm). Hence the diffraction data suggest the TiN arrays are similar in composition to the powdered samples.

(39) Dann, S. E. *Reactions and Characterization of Solids*; Royal Society of Chemistry: Cambridge, U.K., 2000.

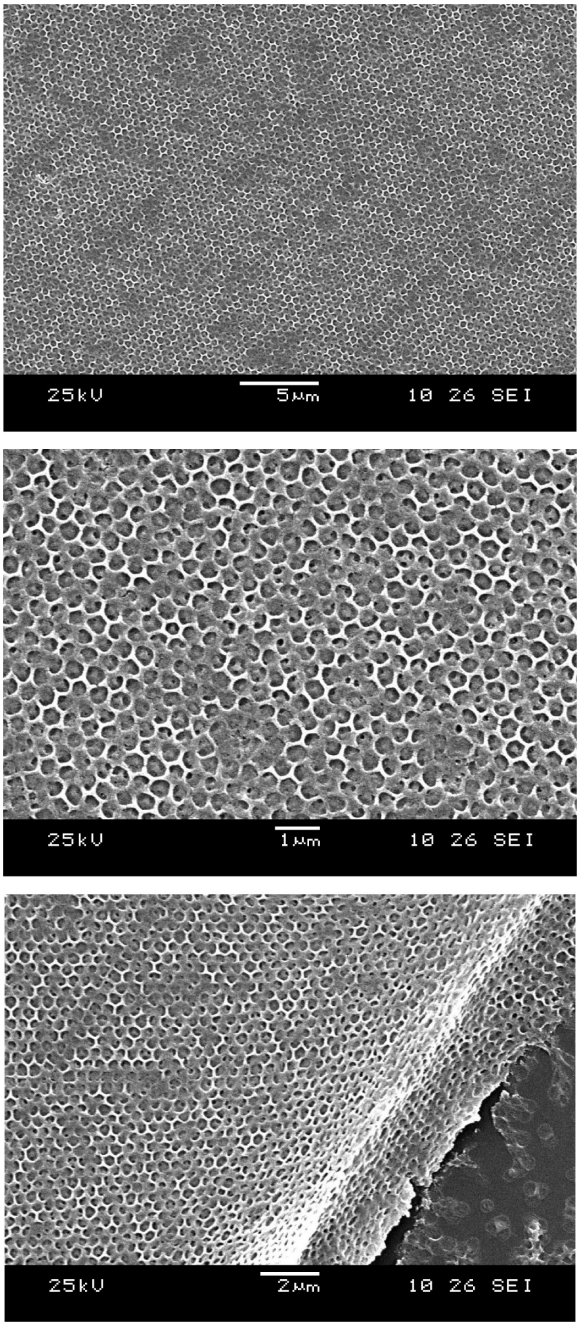

Figure 5. SEM micrographs of thin films of ordered macroporous SiN_x on a silica substrate showing the lack of cracking (top, compare with Figure 2), a highly ordered region (center), and the view down a crack showing that the pores penetrate the depth of the film.

Macroporous SiN_x

Precursor-derived silicon nitride typically varies in composition from Si_3N_4 and here we use the "SiN_x" notation to describe silicon nitride containing low levels of other functional groups similar to the materials often obtained by CVD and used in electronics. Attempts to produce SiN_x precursor sols in hexane, using similar ammonolytic chemistry to that which was recently used to form SiN_x aerogels,[27] were unsuccessful, resulting in

immediate precipitation. This is unsurprising because the chemistry is based on formation of polar Si-NH_2 and Si-NH-Si groups. Si is smaller and less electropositive than Ti and thus the primary amide self-condensation route used above to produce TiN does not work, so SiN_x precursor gels are made with NH_3 as the cross-linking agent. The bridging groups are thus NH_2 and it is unsurprising that solubility of the oligomers in a nonpolar solvent is low. Hence SiN_x arrays were produced by template infiltration of a solid molecular precursor, $Si(NHMe)_4$, dissolved in hexane.

The ammonolysis method adopted involves a slow ramp to 50 °C to encourage reaction between the $Si(NHMe)_4$ and ammonia before heating to 500 °C to decompose the precursor and remove the template. The SiN_x arrays obtained after ammonolysis at 500 °C (Figure 5) suffered less cracks than the TiN ones. Again the ordered macroporous structure is clearly identified, and the porosity extends throughout the structure. These arrays did not exhibit opalescence unless coated (e.g., with gold for the SEM studies). The SiN_x appears to fill the void spaces in the template more effectively than the TiN despite the latter having been deposited from a more concentrated sol (0.57 vs 1.49 mmol cm^{-3}). PXD on the bulk xerogel and the films shows no Bragg scattering, i.e. the SiN_x samples are amorphous. It is likely that sintering of the TiN crystallites reduces the volume of the material in the walls of the macroporous films and it is this process that cracks the films. The SiN_x remains amorphous at these temperatures and thus cracking occurs less and the original spaces between the PS spheres are more fully filled. The alternative explanation is that the cracking is due to a mismatch between the thermal expansion of the material and the substrate or the spheres, and that this mismatch is greater for Ti.

The low density of the amorphous films precluded direct measurements and it was again necessary to investigate bulk xerogels to obtain analytical data. These were produced by heating $Si(NHMe)_4$ under the same conditions as the films. However, it was found that most of the precursor sublimed under these conditions. Mixing the precursor with a dried sample of the PS template and then heating yielded a sample which was shown by microanalysis to contain 41.4% N, 2.2% C, and 2.6% H. This suggests a N-rich silicon nitride (Si_3N_4 would contain 39.9% N) with some residual carbon and hydrogen. Presumably some interaction with the surface capping amidine groups on the PS spheres results in retention of the precursor during heating. The IR spectrum of the bulk SiN_x xerogel reveals the presence of ν_{N-H} (3378 cm^{-1}) and weak ν_{C-H} stretching (2808 and 2900 cm^{-1}). Two typical ν_{Si-N} are present at 1218 and 917 cm^{-1} but no ν_{Si-O} (~1030 cm^{-1}) was observed. The Raman spectrum of the solid revealed only a broad peak at 1430 cm^{-1}, indicating the presence of some elemental carbon. N-rich SiN_x Raman spectra are typically featureless.[40]

The structures obtained are less ordered than ordered macroporous nitrides previously produced by ALD for photonic band gap materials. However, applications such as electrode materials, catalysis and membranes do not require such highly uniform periodic structures. Recently, nanocrystalline TiN has been reported as a potential electrode material for electrochemical capacitors (supercapacitors).[22,41] Using macroporous structures, such as those obtained in the present study, will not only increase the surface area of TiN thin films, but will also allow for effective electrolyte penetration into the structure.

Porous SiN_x materials have shown promising catalytic activity for heterogeneous reactions such as the Knoevenagel reaction.[42] These materials are useful solid base catalysts because of the presence of basic N−H groups in them.[43] Macroporosity may be beneficial if solution phase catalytic reactions, requiring large accessible surface areas and efficient mass transport, were to be carried out. The use of polystyrene templates means that chemical etching using strong acids such as HF, required to remove SiO_2 templates, can be bypassed. This is of great importance for the SiN_x catalytic materials, because HF displaces the active surface N−H groups.[44]

Conclusions

Ordered macroporous TiN and SiN_x thin films were prepared by simple templating methods with polystyrene sphere arrays. Templating of the nitride precursor materials was facilitated by using cross-linked spheres with compatible capping groups and finding precursors that were soluble in hexane, which did not affect the spheres. A sol−gel method was effective for TiN whereas a simple molecular precursor was used for SiN_x. Annealing in ammonia removed the polystyrene template leaving nanocrystalline TiN or amorphous SiN_x with an ordered macroporous (inverse opal) morphology.

Acknowledgment. The authors thank the Egyptian government for a study scholarship (S.H.), the Royal Society for a University Research Fellowship (A.L.H.) and EPSRC (B.M., Grant ref GR/T12286/01) for support. Thanks also to Susanne Huth for collecting the DSC and to Fei Cheng for collecting the Raman data.

(40) Xin, Y.; Huang, X. Z.; Shi, Y.; Pu, L.; Zhang, R.; Zheng, Y. D. *Physica E* **2005**, *30*, 41.
(41) Janes, R. A.; Aldissi, M.; Kaner, R. B. *Chem. Mater.* **2003**, *15*, 4431.
(42) Kaskel, S.; Schlichte, K. *J. Catal.* **2001**, *201*, 270. Hullmann, D.; Wendt, G.; Ziegenbalg, G. *Chem. Eng. Technol.* **2001**, *24*, 147.
(43) Bradley, J. S.; Vollmer, O.; Rovai, R.; Specht, U.; Lefebvre, F. *Adv. Mater.* **1998**, *10*, 938.
(44) Knotter, D. M.; Denteneer, T. J. J. *J. Electrochem. Soc.* **2001**, *148*, F43.